Supplemental material to accompany

Structure and Possible Mechanism of the CcbJ Methyltransferase from *Streptomyces caelestis*[*]

Jacob Bauer,[a†] Gabriela Ondrovičová,[a] Lucie Najmanová,[b] Vladimír Pevala,[a] Zdeněk Kameník,[b] Július Koštan,[c] Jiří Janata,[b] and Eva Kutejová[a,b†]

[*]Submitted to *Acta Crystallogr., Sect. D: Biol. Crystallogr.*

[a]Institute of Molecular Biology, Slovak Academy of Sciences, Dúbravská cesta 21, 845 51 Bratislava, Slovakia

[b]Institute of Microbiology, Academy of Sciences of the Czech Republic, Vídeňská 1083, CZ-142 20 Prague 4, Czech Republic

[c]Department for Structural and Computational Biology, Max F. Perutz Laboratories, University of Vienna, A-1030 Vienna, Austria

[†]To whom correspondence should be addressed:
`evakutej@hotmail.com` or `jacob.bauer@savba.sk`

Supplementary Tables

Table S1: Oligonucleotide primers for point mutants

Mutant	Primer Sequence
Y9F	5′–CTACGACGAGACAACGTTCGGCGACCAGATC–3′
Y17F	5′–CAGATCGCGGACGTCTTCGACGAGTGGC–3′
F117G	5′–CGTCGTCTTCGCGGCGGGCAACACCCTTTTCTGC–3′

Table S2: Docking energies

Substrate	Best Conformation kcal/mol	Docking Energy Range kcal/mol
N-demethyl celesticetin	-8.7	-8.7 – -8.0
[H-N-demethyl celesticetin]$^+$	-8.8	-8.8 – -8.1
celesticetin	-7.6	-8.4 – -7.1
[H-celesticetin]$^+$	-8.2	-8.7 – -7.4
N, O-didemethyl celesticetin	-7.5	-7.7 – -7.0
[H-N, O-didemethyl celesticetin]$^+$	-7.8	-8.4 – -7.7
O-demethyl celesticetin	-7.5	-7.9 – -7.3
[H-O-demethyl celesticetin]$^+$	-8.0	-8.8 – -7.9
N-demethyl desalicetin	-6.5	-6.5 – -5.5
[H-N-demethyl desalicetin]$^+$	-6.7	-7.1 – -6.2
desalicetin	-6.8	-6.8 – -5.8
[H-desalicetin]$^+$	-6.8	-6.8 – -5.9
N, O-didemethyl desalicetin	-6.3	-6.5 – -5.8
[H-N, O-didemethyl desalicetin]$^+$	-6.8	-7.1 – -6.6
O-demethyl desalicetin	-6.5	-6.5 – -5.9
[H-O-demethyl desalicetin]$^+$	-6.2	-6.9 – -6.1
N-demethyl lincomycin	-7.3	-7.9 – -6.5
[H-N-demethyl lincomycin]$^+$	-7.3	-7.7 – -6.6
lincomycin	-7.0	-8.1 – -7.0
[H-lincomycin]$^+$	-8.0	-8.0 – -7.3

Supplementary Figures

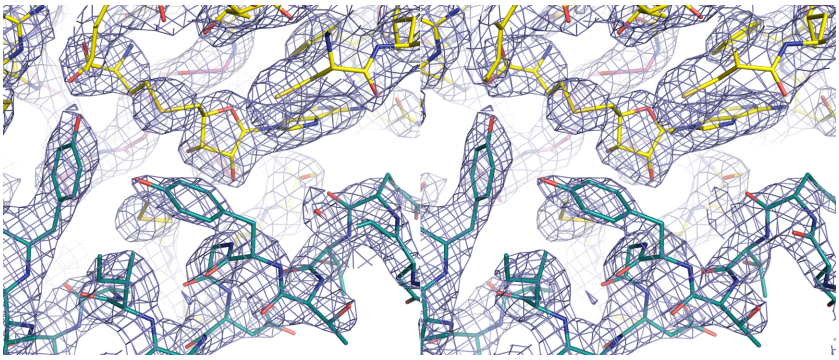

Figure S1: A stereoview of a weighted $2F_o - F_c$ electron density map of the CcbJ–SAH complex at a contour level of 1.5σ (corresponding to 0.310 $e/\text{Å}^3$) showing the co-factor binding site and bound SAH. Residues 5–17 (in the foreground colored blue) are ordered in the CcbJ–SAH complex, but not in the native structure.

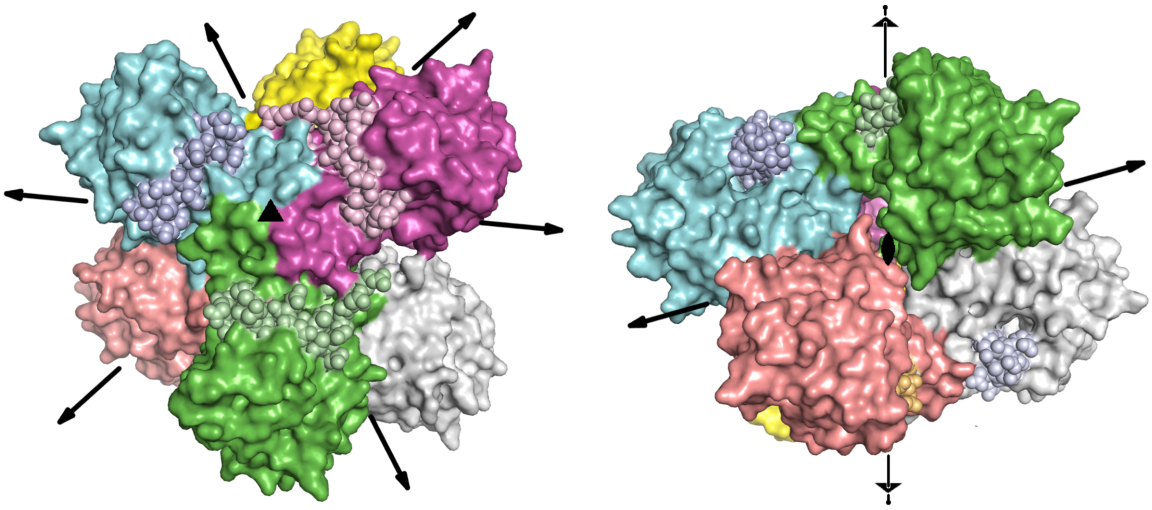

Figure S2: An overview of the CcbJ hexamer showing the non-crystallographic symmetry elements. The left-hand view is down the 3-fold axis and perpendicular to the three 2-fold axes (arrows). The right-hand view is down one of the 2-fold axes (the right-hand view may be obtained from the left-hand view by rotating the left-hand image 90° about the horizontal axis, followed by a 45° rotation about the vertical axis). The residues shown as spheres are those which are disordered in the native and SeMet structures, but can be traced in the CcbJ–SAH complex.

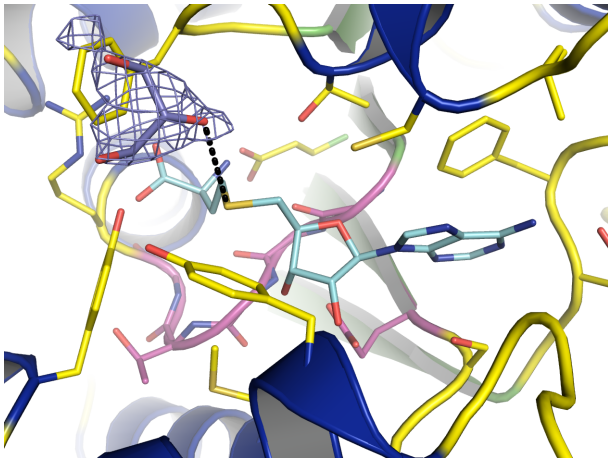

Figure S3: An illustration of one of the glycerol molecules which appear to be present in the substrate binding cavity of the CcbJ–SAH complex structure. The orientation of the complex in this figure matches that of the SAH binding site shown in Figure 5 in the main text. The weighted $2F_o - F_c$ electron density map shown around the glycerol is at a contour level of 1.5σ (corresponding to 0.310 $e/\text{Å}^3$). The distance between the glycerol hydroxyl group nearest the SAH Sδ atom indicated by the dashed line is 5.3 Å. This is a closer approach than would be possible if the Cϵ atom of SAM were present.

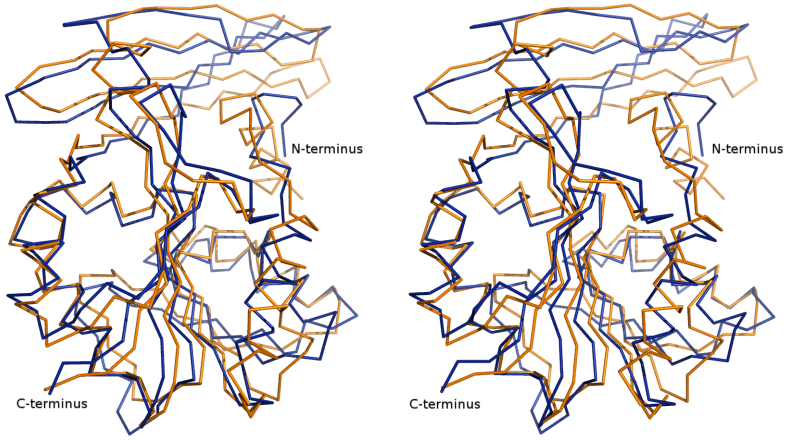

Figure S4: A stereoview showing a Cα overlay of the native CcbJ structure (blue) with the uncharacterized methyltransferase from *C. acetobutylicum* (PDB ID 1Y8C).

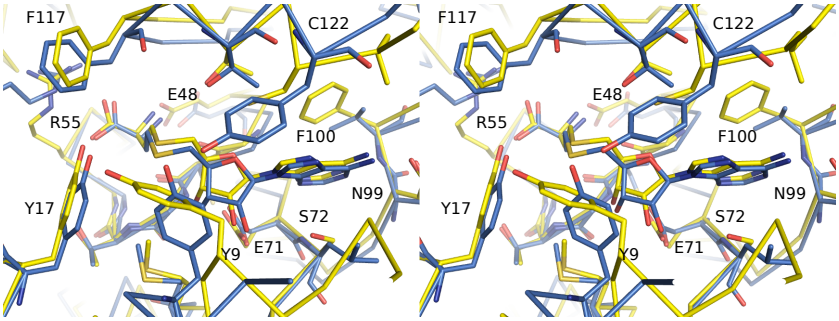

Figure S5: A stereoview showing the overlap of the co-factor binding sites of the CcbJ–SAH complex (yellow) with the uncharacterized methyltransferase from *P. horikoshii* OT3 (PDB ID 1WZN; slate blue). Note that there are counterparts for Tyr-9, Tyr-17, Glu-48, Arg-55, Phe-117, and Asn-99. The identity is not complete, however, since Cys-122, Phe-100, and Ser-72 have been replaced with a tyrosine, a valine, and a leucine, respectively.

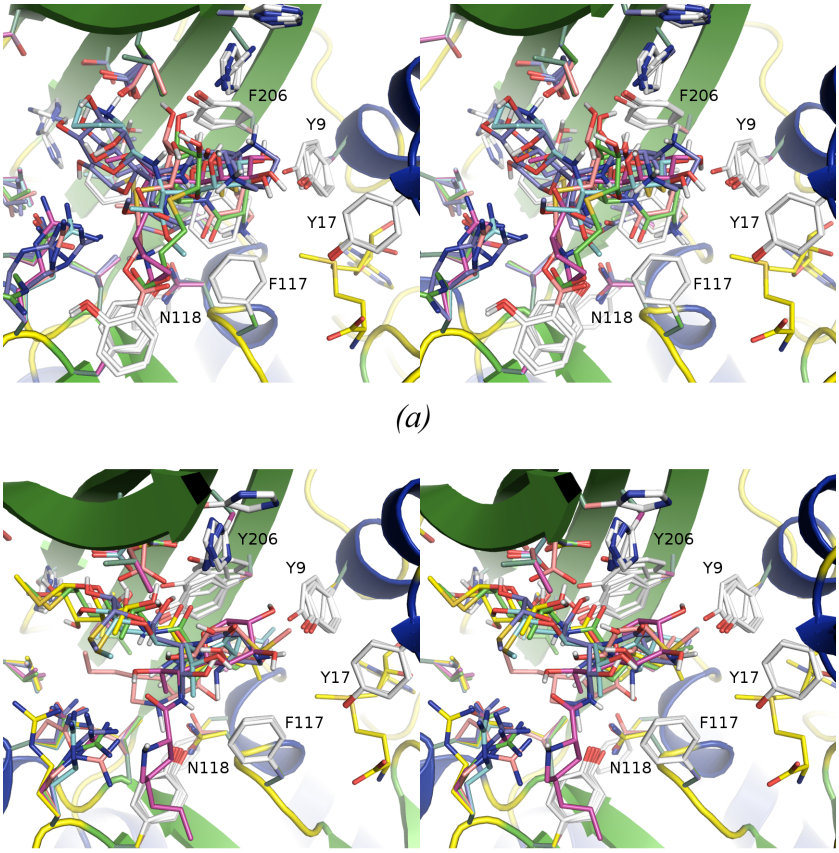

Figure S6: Clustering of the top six docking solutions of protonated *N*-demethylcelesticetin (a) and *N*-demethyllincomycin (b).

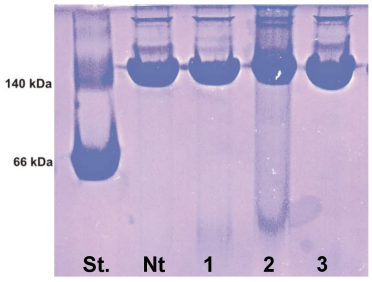

Figure S7: The oligomeric structure of purified wild-type and mutant CcbJ proteins was compared using blue native polyacrylamide gel electrophoresis. All proteins except the BSA standard possess an N-terminal hexahistidine tag. Samples: St—BSA molecular weight standard, Nt—purified native CcbJ protein, Lane 1—F117G, Lane 2—Y9F, and Lane 3—Y17F.

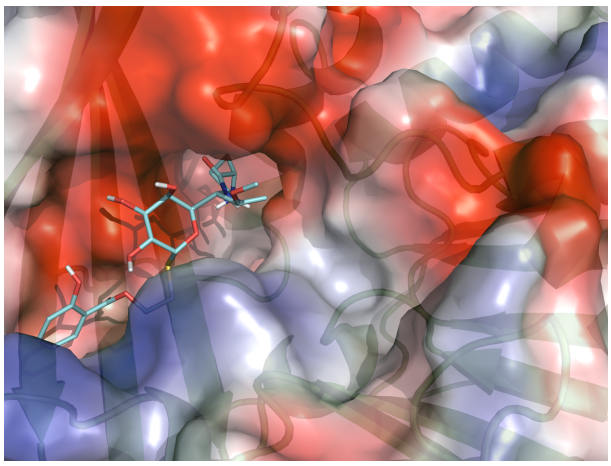

Figure S8: A view showing the electrostatic surface of the CcbJ active site. A docked protonated, *N*-demethylcelesticetin is shown at center for reference. Note that the surface corresponding to the active site cover (the antiparallel β-sheet) is more negatively charged than the side opposite.

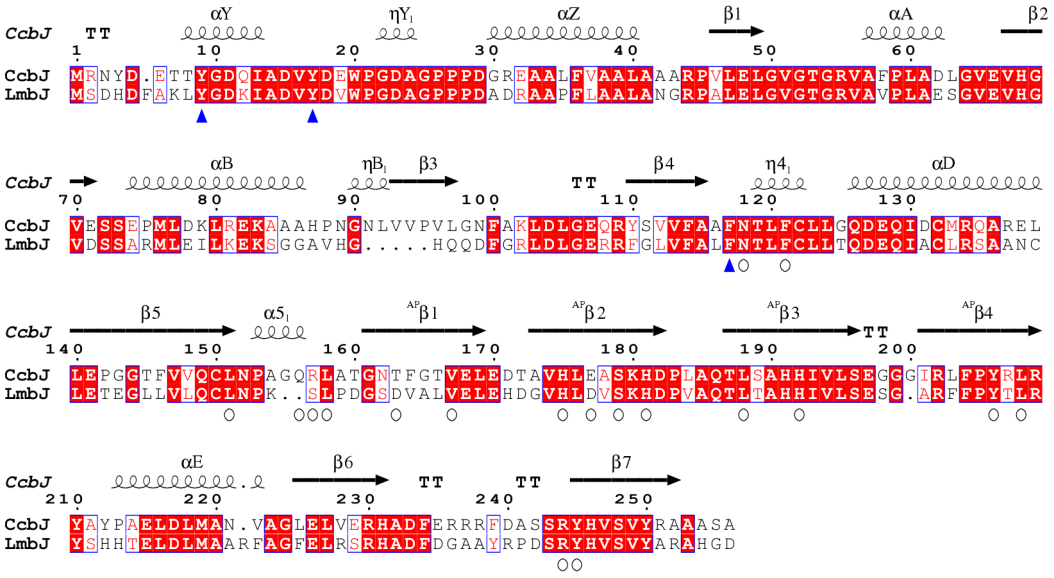

Figure S9: Pairwise sequence alignment between CcbJ and LmbJ. Identical residues are highlighted. Tyr-9, Tyr-17, and Phe-117 are indicated by blue triangles below the alignment while open circles mark the positions of those residues which are predicted to make contact with the substrate. Secondary structural elements are noted at the top (η denotes a 3_{10} helix and TT a hydrogen-bonded turn). The alignment was prepared using ClustalX2 (Larken *et al.*, 2007) and the picture, with ESPript 2.2 (Gouet *et al.*, 1999).

References

Larkin, M. A., Blackshields, G., Brown, N. P., Chenna, R., McGettigan, P. A., McWilliam, H., Valentin, F., Wallace, I. M., Wilm, A., Lopez, R., Thompson, J. D., Gibson, T. J. & Higgins, D. G. (2007). *Bioinformatics* **23**, 2947–2948.

Gouet, P., Courcelle, E., Stuart, D. I. & Métoz, F. (1999). *Bioinformatics* **15**, 305–308.